A finite element model investigating the cyclic strains in the lamina cribrosa and their potential role in glaucoma

Omkar G. Kaskar[1], David Fleischman[2], Andrey V. Kuznetsov[1], Landon Grace[1]

[1]Mechanical and Aerospace Department, North Carolina State University, Raleigh, NC, USA; [2]Department of Ophthalmology, University of North Carolina at Chapel Hill, Chapel Hill, NC, USA

Abstract

Purpose: To present the cyclic strains developed in the lamina cribrosa due to the cardiac cycle-driven fluctuations in the pressure conditions around the optic nerve head.

Design: Finite element analysis on 3-D models of the human eye.

Methods: Varying intraocular pressure and cerebrospinal fluid pressure over a cardiac cycle were provided as boundary conditions in the finite element models. The cyclic strains generated in the lamina cribrosa were compared at different mean intraocular pressures representing normal and pathological conditions.

Results: The peak maximum principal strains varied from 0.7% to 1.4% across all cases of normal and elevated intraocular pressure, and occurred along the periphery of the lamina cribrosa. The amplitude of the cyclic strains in the lamina cribrosa increased by 3.5% from the normal case to the pathological cases. The amplitudes did not change significantly for the pathological cases with mean intraocular pressures of 21.6 mmHg, 26.6 mmHg, and 31.6 mmHg.

Conclusion and future perspective: The effect of short-term pressure changes on the tissues of the optic nerve head has not been studied extensively. *In vitro* and *ex vivo* experiments can be designed based on the results of computational studies to observe the effect of cyclic strains on mechanosensitive cells in the optic nerve head. Furthermore, the repetitive impact of cyclic strains in the lamina cribrosa

Correspondence: Landon Grace, Mechanical and Aerospace Engineering Department, North Carolina State University, 911 Oval Drive, Raleigh, NC 27695, USA.
Email address: landon_grace@ncsu.edu

over numerous cardiac cycles gives rise to the possibility of mechanical fatigue contributing to the structural damage around the optic nerve head. A cumulative damage model can be developed based on the results of this study.

Keywords: cerebrospinal pressure fluctuations, fatigue, finite element analysis, glaucoma, intraocular pressure fluctuations

1. Introduction

Primary open-angle glaucoma (POAG) is characterized by progressive damage to the optic nerve head (ONH), which results in visual field loss.[1] Glaucoma is the leading cause of irreversible blindness worldwide, yet the contributing factors and mechanisms of damage progression remain poorly understood. The ONH is anteriorly exposed to the intraocular pressure (IOP), and posteriorly to the cerebrospinal fluid (CSF) pressure in the retrobulbar subarachnoid space (RSAS). Figure 1 shows a simplified anatomy of the posterior portion of the eye with the pressures acting on the different tissues. The mechanical theory of glaucomatous optic neuropathy suggests that the elevated IOP results in stresses that the laminar beams cannot withstand, leading to their collapse and the posterior bowing of the lamina cribrosa.[2] Furthermore, the axons of the retinal ganglion cells that pass through the lamina cribrosa are damaged either directly due to the increased pressure or from the strains developed in the tissues.[2-5] This restricts axoplasmic flow transport, which might eventually lead to cell death causing glaucomatous
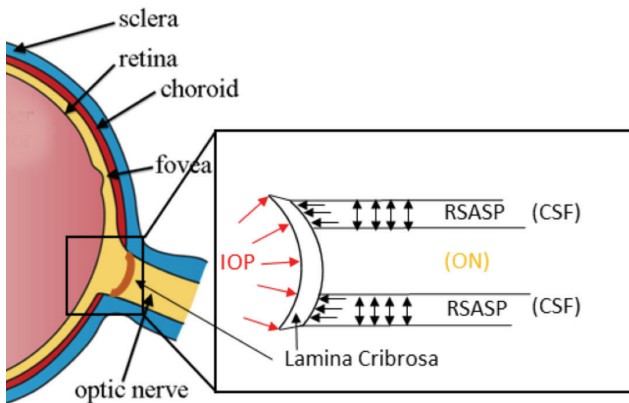
Fig. 1. Anatomy of the posterior part of the human eye. Intraocular pressure (IOP) acts on the anterior portion of the lamina cribrosa. Cerebrospinal fluid (CSF) in the subarachnoid space around the ON (optic nerve), immediately posterior to the eye, exerts a pressure on the lamina cribrosa, called the retrobulbar subarachnoid space pressure (RSASP).

optic neuropathy.

The two pressures, RSAS pressure and IOP, are dynamically changing pressures that are affected by the cardiac cycle, diurnal variations, and episodic elevations.[6] As seen from the compartmental model developed in our previous study,[7] and as observed by Morgan *et al.*,[8] there is an offset in the peak of the IOP curve and the CSF pressure curve over a cardiac cycle. This would result in a complex cyclic load on the ONH tissues. The effect of IOP fluctuations and its role in glaucoma progression using functional indicators such as visual fields has been studied previously. However, the structural biomechanical response of the ONH to the combined loading of changing RSAS pressure and IOP has not yet been presented. It has even been suggested that one of the reasons for the poor understanding of the role of IOP in the development of glaucoma is the clinical measurement of IOP—a static representation of a dynamic phenomenon that fails to capture the potentially more damaging fluctuations in pressure.[9]

The current study computationally explores the impact of cardiac cycle-driven fluctuations in IOP and RSAS pressure on the ONH tissues using finite element (FE) analysis. In a recent study, Jin *et al.* used FE models to investigate the origins of the cardiac cycle-driven fluctuations in IOP and their effects on the biomechanics of the ONH.[10] Previously, generic as well as patient-specific FE models have assumed constant pressure conditions while studying the biomechanics of the ONH.[11-25] Earlier models evaluated the stresses induced at physiological and elevated levels of IOP using idealized geometry and assuming linear elastic tissue properties.[11-13] The models were then updated to include the anatomy of the ONH in greater detail and with more realistic boundary conditions to evaluate the influence of geometric factors as well as material properties on the generated stresses.[14-18] While the earlier models focused exclusively on evaluating IOP-induced stresses, more recent models have studied the effects of CSF pressure acting in conjunction with IOP.[18,19,21,23-25] In the current study, we have reported the likely strains developed in the ONH tissues as the IOP and RSAS pressure change over a cardiac cycle. We further explore the effects of these fluctuations at elevated levels of IOP.

2. Methods

A 3-D, generic, axisymmetric model of the ONH and surrounding tissues was developed as follows:

2.1. Geometry
The 3-D geometry, as shown in Figure 2, was modeled in Solidworks® (Dassault Systèmes SOLIDWORKS Corp. Waltham, MA, USA) using the anatomical details of the human eye specified in previous studies.[12,13,23] The model comprised the scleral tissue, lamina cribrosa, prelaminar neural tissue, and the optic nerve,
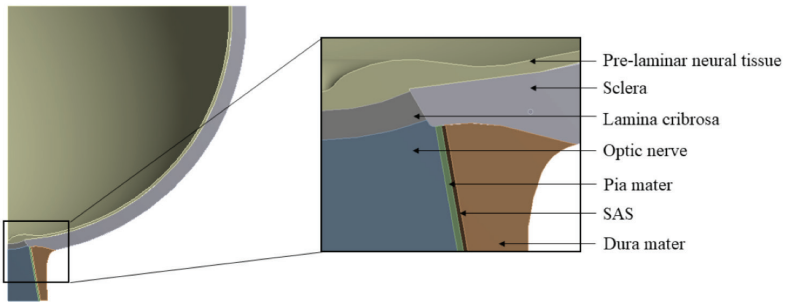
Fig. 2. Axisymmetric 3-D model of the human eye highlighting the tissues of the optic nerve head.

which included the pia mater and dura mater. The baseline geometric details as highlighted in *Sigal et al.*[13] were used to model the sclera, lamina cribrosa, prelaminar neural tissue, optic nerve, and pia mater. Additionally, following the study by Hua *et al.*,[23] the subarachnoid space (SAS) and the dura mater were also included. The SAS extended along the optic nerve posterior to the globe, and was assumed to have a constant thickness of 0.05 mm. [23] Similar modeling studies[19-21,23] have used values ranging from 0.2–0.5 mm for the thickness of the dura mater based on previously reported experimental values.[26,27] In the present model, the dura mater thickness at the base was considered to be an averaged value of 0.35 mm, with subsequent thickening at the scleral junction.

2.2. Material properties

The neural tissue, pia mater, and dura mater were assumed to be linearly elastic and isotropic. As such, the Young's modulus and the Poisson's ratio were the only material properties required to completely determine the mechanical response of these structures. These tissues were assumed to be nearly incompressible with a Poisson's ratio of 0.49.[13] The Young's moduli for each of these tissues were: 0.03 MPa for the neural tissue, 3 MPa for the pia mater, and 4 MPa for the dura mater.[13,23]

A nonlinear, isotropic, hyperelastic material model was used to describe the lamina cribrosa and the scleral tissue. The first order Ogden model was fitted to the uniaxial stress-strain data available for human scleral tissue[28] used by Tong *et al.*[24] in their FE study to define the material properties for the sclera. Similarly, the uniaxial stress-strain data for the control specimen of the human lamina cribrosa[29] was used to evaluate the first order Ogden model parameters (μ_1(Pa), α_1). Figure 3 shows the uniaxial stress-strain experimental data for human sclera and lamina cribrosa. The following material parameters were determined through curve fitting the experimental data using the engineering data module in ANSYS Workbench: for sclera, μ_1= 15818 Pa and α_1= 56.8; and for lamina cribrosa, μ_1 = 3.6 x 105 Pa and α_1= 10.4.

a

b
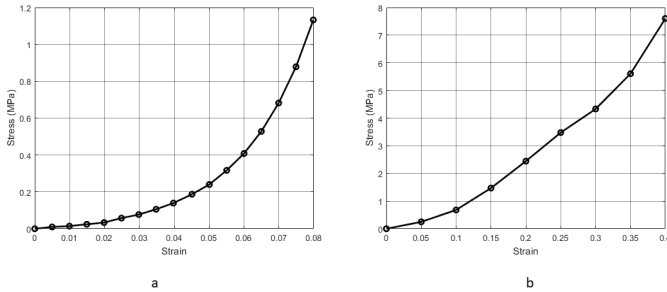
Fig. 3. Uniaxial stress-strain experimental data for human (*a*) sclera[28] and (*b*) lamina cribrosa.[29]

2.3. Boundary conditions

The fluctuating IOP and RSAS pressure over a cardiac cycle, derived from the previously developed compartmental model,[7] are shown in Figure 4. The IOP was applied over the internal surface of the eye, while the RSAS pressure was specified along the SAS, as shown in Figure 5. The CSF pressure, acting immediately posterior to the ONH in the RSAS, is often different from the intracranial or spinal (lumbar puncture) pressure.[30-33] However, since the experimental quantification of this pressure has not been done, previous models have considered the CSF pressure to be equal to the clinically available estimates of intracranial pressure obtained through a lumbar puncture.[19-21] Moreover, the RSAS pressure is affected by multiple factors such as the resistance to the CSF flow due to the complex internal architecture of the optic nerve SAS and the lymphatic outflow of CSF from this region.[7] The external pressure on the globe and the dura mater is equivalent to the physiological orbital tissue pressure, which is assumed to be a constant value of 2 mmHg.[34] A frictionless support boundary condition was specified at the equator
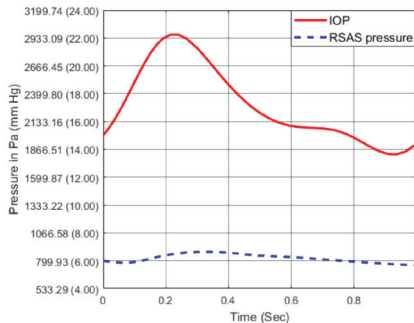
Fig. 4. Intraocular pressure (IOP) and retrobulbar subarachnoid space (RSAS) pressure curves over a cardiac cycle.
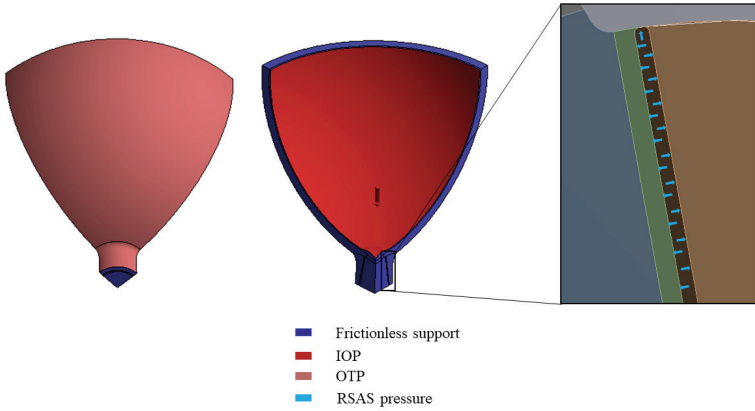
Fig. 5. Boundary conditions imposed on the different surfaces in the finite element model.

and the symmetry planes. This restricted the eye globe movement in the circumferential and meridional directions, while allowing the globe to move freely in the radial direction. A frictionless support was applied at the base of the optic nerve and sheath, which restricted its movement in the anterior-posterior direction. The interfaces between the different tissues were modeled as bonded contacts, which prevented any slipping or separation of the tissues. Figure 5 summarizes the boundary conditions applied to the model.
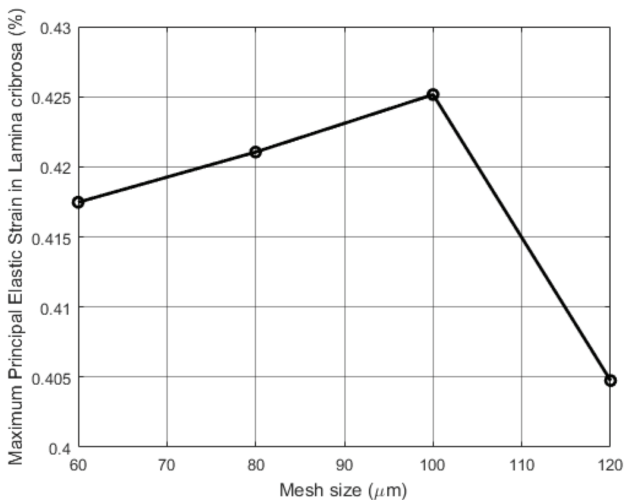
Fig. 6. Mesh convergence showing the maximum principal strains in the lamina cribrosa for different mesh sizes.

2.4. Numerical approach

A commercial FE software, ANSYS® Academic Research Mechanical, Release 19.2 (ANSYS Inc. Canonsburg, PA, USA), was used to solve the model. An implicit, quasi-static simulation for IOP and RSAS pressure over a single cardiac cycle was carried out. An initial time step of 0.1 seconds was provided which could be increased to 0.2 seconds to achieve faster convergence. A quadratic, 20-node hexahedral element dominated mesh was generated with additional tetrahedral, pyramid, and wedge elements to capture the irregular geometry. A mesh convergence study as described in Shin *et al.*[22] was followed to achieve the necessary resolution in the critical regions of interest. The maximum principal strains developed in the lamina cribrosa were evaluated for different mesh sizes from 120 μm to 60 μm, in steps of 20 μm, as shown in Figure 6. This was done until the difference in the values of the maximum principal strains between two consecutive mesh sizes was less than 3%. Based on the convergence study, the size of the elements in the lamina cribrosa was set to 80 μm. The size of the elements in the pia mater was fixed at 20 μm, while the size in the dura mater and optic nerve was 80 μm. The sclera and the prelaminar neural tissue had elements sized 100–300 μm, with a greater density of elements concentrated near the ONH region. The overall model was solved for a mesh with 464,883 nodes and 164,625 elements.

3. Results

As shown in *Table 1*, a baseline case with physiologically normal mean IOP and RSAS pressure was simulated, while the cases 1, 2, and 3 replicated conditions of elevated IOP, which has long been considered a risk factor for glaucomatous optic nerve damage.[35,36]

The peak values of the maximum principal strain for all the models varied from 4.2% to 7.9% and occurred in the prelaminar neural tissue. Sigal *et al.*[13] and Hua *et al.*[23] in their FE models have reported strains greater than 5% in the tissues around the optic nerve, and have noted that a similar range of strain values were observed in some *ex vivo* human and porcine models, even with their simplification of linear, elastic, and isotropic tissue properties.

Scanning electron microscopic examination of human ONH,[5] as well as experimental animal models[3,4] have shown that glaucomatous damage generally occurs at the level of the lamina cribrosa. Therefore, we have focused on the strains generated in the lamina cribrosa over a cardiac cycle. The peak maximum principal strains varied from 0.7% to 1.4%, as shown in Figure 7, across the range of IOP levels chosen for the present study.
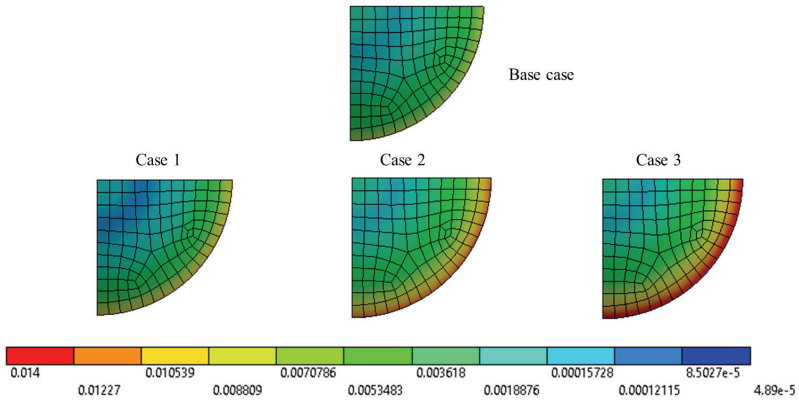
Fig. 7. Variation of the maximum principal strains in the lamina cribrosa along the radial direction under the three different pathological cases and the physiologically normal base case. Base case: intraocular pressure (IOP) = 2,211.82 Pa (16.59 mmHg), retrobulbar subarachnoid space pressure (RSASP) = 814.60 Pa (6.11 mmHg); Case 1: IOP = 2,878.43 Pa (21.59 mmHg), RSASP = 814.60 Pa (6.11 mmHg); Case 2: IOP = 3,545.84 Pa (26.59 mmHg), RSASP = 814.60 Pa (6.11 mmHg); Case 3: IOP = 4,211.65 Pa (31.59 mmHg), RSASP = 814.60 Pa (6.11 mmHg).
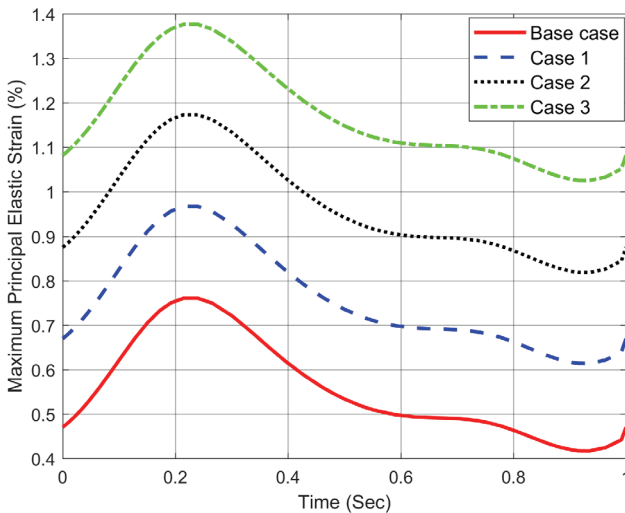
Fig. 8. Peak values of maximum principal strains in the lamina cribrosa under the three different pathological cases and the physiologically normal base case. Base case: intraocular pressure (IOP) = 2211.82 Pa (16.59 mmHg), retrobulbar subarachnoid space pressure (RSASP) = 814.60 Pa (6.11 mmHg); Case 1: IOP = 2,878.43 Pa (21.59 mmHg), RSASP = 814.60 Pa (6.11 mmHg); Case 2: IOP = 3,545.84 Pa (26.59 mmHg), RSASP = 814.60 Pa (6.11 mmHg); Case 3: IOP = 4,211.65 Pa (31.59 mmHg), RSASP=814.60 Pa (6.11 mmHg).
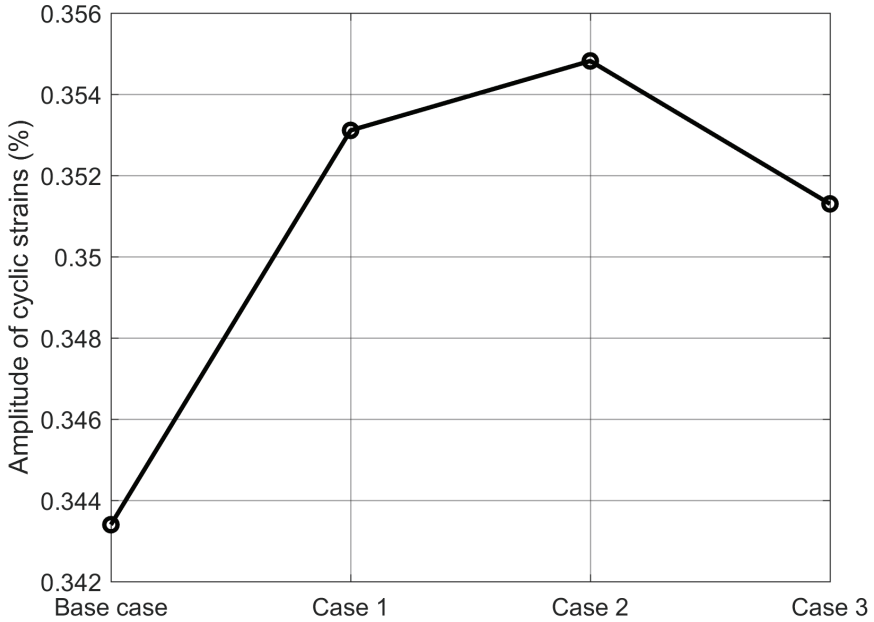
Fig. 9. Amplitude of the cyclic strains in the lamina cribrosa increases from the physiologically normal base case to the pathological cases. Base case: intraocular pressure (IOP) = 2,211.82 Pa (16.59 mmHg), retrobulbar subarachnoid space pressure (RSASP) = 814.60 Pa (6.11 mmHg); Case 1: IOP = 2,878.43 Pa (21.59 mmHg), RSASP = 814.60 Pa (6.11 mmHg); Case 2: IOP = 3,545.84 Pa (26.59 mmHg), RSASP = 814.60 Pa (6.11 mmHg); Case 3: IOP = 4,211.65 Pa (31.59 mmHg), RSASP = 814.60 Pa (6.11 mmHg).

Table 1. Mean pressures over a cardiac cycle for the different cases

Case	Description	Mean IOP in Pa (mmHg)	Mean RSAS pressure in Pa (mmHg)
Base case	Normal IOP and RSAS pressure	2,212 (16.6)	815 (6.1)
Case 1	Elevated IOP and normal RSAS pressure	2,878 (21.6)	815 (6.1)
Case 2	Elevated IOP and normal RSAS pressure	3,545 (26.6)	815 (6.1)
Case 3	Elevated IOP and normal RSAS pressure	4,212 (31.6)	815 (6.1)
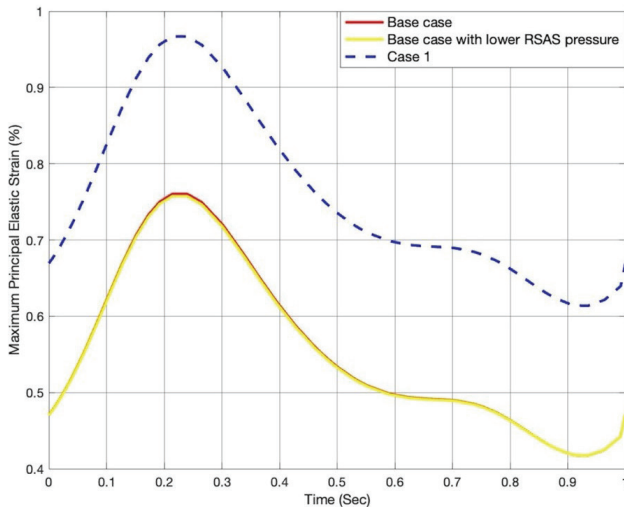
Fig. 10. Peak values of maximum principal strains in the lamina cribrosa for Base case: intraocular pressure (IOP) = 2,211.82 Pa (16.59 mmHg), retrobulbar subarachnoid space pressure (RSASP) = 814.60 Pa (6.11 mmHg); Base case with lower RSAS pressure: IOP = 2,211.82 Pa (16.59 mmHg), RSASP = 146.65 Pa (1.11 mmHg); Case 1: IOP = 2,878.43 Pa (21.59 mmHg), RSASP = 814.60 Pa (6.11 mmHg).

The peak values of the maximum principal strains generated over a cardiac cycle under the different pressure conditions are shown in Figure 8. As expected, the magnitude of the strains averaged over the cardiac cycle increased from 0.5% in the base case to 1.2% in case 3. The maximum values of the strain were 1.2–1.4 times higher than the average strain over the cardiac cycle across all cases. As shown in Figure 9, the amplitude of the cyclic strains increased by 3.5% from the base case to case 1, thereafter remaining relatively similar across the three pathological cases.

An additional case with the physiological level of mean IOP and lower RSAS pressure was simulated. Studies have shown that an increased difference between these two pressures (translaminar pressure difference) may be an independent risk factor for glaucoma.[37] The simulation was carried out with a mean IOP equivalent to the base case at 2,211.82 Pa (16.59 mmHg) and a lower RSAS pressure of 146.65 Pa (1.11 mmHg). Figure 10 shows the peak values of maximum principal strains developed in the lamina cribrosa for the simulation with lower mean RSAS pressure compared with the base case and pathological case 1. The cyclic strains developed in the base case with RSAS pressure equal to 814.60 Pa (6.11 mmHg) and lower RSAS pressure of 146.65 Pa (1.11 mmHg) were similar. Additionally, although the translaminar pressure difference for the base case with lower RSAS pressure of 146.65 Pa (1.11 mmHg) and pathological case 1 were similar, the cyclic strains developed were different and are the result of the increased IOP.

4. Discussion

In the present study, we have shown the variation of the strains within the lamina cribrosa as the IOP and RSAS pressure change over a cardiac cycle. As seen in Figure 7, the highest principal strains are observed at the periphery of the lamina cribrosa under all pressure conditions. The increased peripheral strains are attributed by Jonas *et al.*[38] to the anatomy of the ONH. The increased backward bowing of the lamina cribrosa along the periphery as compared with the center might be due to the optic nerve, which is immediately posterior to the lamina cribrosa. The regions in the lamina cribrosa facing the central trunk of the optic nerve may have less pronounced backward bowing in contrast to the outer regions, which are closer to the CSF space.

The translaminar difference does not seem to have a significant effect on the cyclic strains, as seen in Figure 10. This suggests that the strains developed in the lamina cribrosa are dependent on the IOP. However, a much more detailed analysis would be required to make a definitive conclusion. Retrospective and prospective studies performed thus far have shown that the RSAS pressure was lowered in subjects with POAG. Burgoyne[39] suggested that the glaucomatous damage to the retinal ganglion cell axons may not necessarily occur at locations with the highest strains. Instead, as the strains increase in the ONH tissues, axon physiology may break down at locations where the translaminar pressure difference is high.

Purely from a structural point of view, the cyclical strains induced in the lamina cribrosa present the possibility of mechanical fatigue contributing to the structural damage of the laminar beams. Mechanical fatigue is characterized by structural failure resulting from accumulated damage by the action of repeated loads that do not exceed a particular material's yield strength. The cyclic strains over each individual cardiac cycle may not be high enough to induce structural damage, but their cumulative effect over repetitive cycles might contribute to the damage of laminar beams. As seen in Figure 9, the amplitude of the cyclic strains increased under pathological conditions. This may have implications for the aggressive progression of glaucoma in individuals with higher IOP, as shown by Jay and Murdoch in their longitudinal study to estimate the progression by testing visual field loss.[40] Mechanical damage due to repeated loads on the ONH may explain the progressive nature of damage to the tissues that is a hallmark of this disease. Patient age has been documented as a significant risk factor and the occurrence of glaucoma is known to increase with age.[41] This implies that cumulative exposure to pathological conditions likely play a role in the development of the disease. Cumulative damage models taking into account natural ageing and the self-healing nature of body tissues may provide valuable insight into the progression of ONH tissue damage and associated visual field loss. The lamina cribrosa and sclera are known to actively remodel under IOP-driven strains. The remodeling results in changes in tissue anisotropy, an increase in connective tissue volume, tissue migration, and

elongation or shortening of tissues.[42] Computational models have been proposed to reproduce individual remodeling processes and these can be integrated with the current approach in future studies. While the mitigating effect of tissue remodeling may theoretically preclude failure of tissues from mechanical fatigue only, there are other factors that might contribute to the accumulated damage in the ONH tissues. Studies have indicated that the sclera and lamina cribrosa stiffen with age, changing the biomechanical response of the ONH.[43,44] While the stiffening of the sclera and lamina cribrosa might be viewed as a protective measure to resist mechanical strain, it also induces larger IOP spikes due to the decreased compliance of the tissues, making them more susceptible to damage.[9] Moreover, diurnal and episodic elevations in IOP will also likely lead to repeated strains. Additionally, in a recent modeling study, Wang *et al.*[20] have shown that the horizontal movement of the eye causes large strains in the ONH tissues and have suggested that these transient strains could have a long-term effect because of how frequently we move our eyes for daily activities.

Mechanical fatigue damage due to overuse or poor healing response of tissues has been attributed to injuries in tendons and ligaments.[45] However, the effect of mechanical fatigue has not yet been investigated in ONH tissues. Few constitutive models have been proposed for fatigue damage in soft biological tissues.[46-48] Specifically, constitutive models for bioprosthetic heart valves have been proposed.[48] These models mimic fatigue-induced damage in collagenous tissues, leading to irreversible uncrimping of the collagen fibers (permanent set) and progressive damage to fibrils, which decreases the stiffness of the tissue (stress softening). Computational simulations utilizing fatigue damage constitutive models calibrated via experimental tests could be useful in investigating the damage mechanism in the ONH and its contribution to the development of glaucoma. Like tissue fatigue studies related to musculoskeletal and cardiovascular applications, this approach is currently hindered by the lack of experimental data. Fatigue experiments focusing on generating data under different loading conditions and over a varying number of cycles would be required to properly calibrate the existing constitutive models.

Although IOP is a well-acknowledged risk factor for glaucoma, and currently the only modifiable one for its management, IOP fluctuations and their role in the pathophysiology of glaucoma remains an active area of interest. Animal studies have measured diurnal IOP fluctuations of approximately 667 Pa (5 mmHg), and much higher fluctuations of approximately 200–5,333 Pa (15–40 mmHg) on the timescale of seconds.[9,49] In humans, while some studies have demonstrated that IOP fluctuations over all timescales are potential risk factors for glaucoma,[50-56] others have found no correlation between the two.[57,58] Analogous to IOP fluctuations, transient changes in the CSF pressure have also been hypothesized to play a role in the progression of glaucoma.[6,59] Further, it has been suggested that pulsatile loads have a more significant effect on cell physiology than constant mechanical loads[6,60-62] and the cells in the ONH are much more susceptible to react to the short-term changes

in pressure than the overall slower changes in the mean pressures.[61] Kirwan *et al.*[62] found that lamina cribrosa cells respond to cyclical mechanical strains by transcription of modulators and components of the extracellular matrix. Similar experimental studies can be designed based on computational studies such as ours to investigate the effect of short-term pressure changes.

There are certain limitations in the current study that need to be addressed to develop more sophisticated models in the future. Although the dynamic pressure conditions are prevalent in all eyes, strains developed in the lamina cribrosa are derivative of the eye-specific morphology and tissue stiffness. Thus, there is a possibility that the magnitude of strain is higher in some eyes, making them more susceptible to damage.[61] Numerous studies have pointed to factors such as stiffness of the tissues and their anatomy to significantly affect the stresses and strains predicted within them.[12,13,16,23,25] This variability is difficult to capture in a generic model. Another limitation of the current model is the assumption of hyperelastic material properties for the lamina cribrosa and the sclera, and linearly elastic properties for the remaining tissues. In reality, these tissues have a non-linear and highly anisotropic behavior. However, other FE models have also included these simplifications since they constitute a reasonable approximation of the large-scale behavior of the tissues.[11-13,21,23,24] Previous computational studies have suggested that the anisotropy of the scleral region reduces the expansion of the scleral canal, thereby protecting the tissues of the ONH.[63] Other studies have shown that glaucomatous eyes exhibit a lower degree of scleral anisotropy.[64] However, detailed studies would be required to determine whether the decreased anisotropy is an effect or a cause of the onset of glaucoma. Additionally, viscoelastic effects were not included. Altered rates of change of the dynamic pressure conditions around the ONH would likely affect the biomechanical response of the tissues. Viscoelasticity has been shown to reduce dynamic stresses and strains developed in arterial walls, having implications of mitigating fatigue damage in arteries.[65] Lastly, we have considered the effect of cardiac cycle-driven changes in the IOP and RSAS pressure in isolation. The effect of body posture on the pressures is not investigated; the IOP and RSAS pressure curves are obtained assuming supine position. Over any given length of time, the stresses and strains generated in the ONH would likely be more complex.

5. Conclusion

The pressure conditions around the ONH tissues are critical to understanding the cause and progression of glaucoma. This is further compounded by the fact that the two pressures acting in this region, IOP and CSF pressure, are dynamically changing. Thus, a static measure of pathophysiological pressure conditions to evaluate their impact on the ONH tissues leading to glaucoma may not suffice. Therefore, in the current study we have presented the cyclic strains developed in ONH tissues, specif-

ically the lamina cribrosa, due to cardiac cycle-driven pressure changes.

A FE analysis of a generic model of the human eye was carried out. Mechanical loads induced by dynamic IOP and CSF pressure changes over a cardiac cycle were applied. It was observed that both mean cyclic strains and strain amplitudes increased under pathological IOP conditions. The results can be used to develop *in vitro* experiments to understand the impact of short-term pressure fluctuations on the mechanosensitive cells of the lamina cribrosa. Furthermore, the contribution of mechanical fatigue in the structural damage of the ONH can be investigated. Cumulative damage models due to repetitive strains that account for the characteristics of living tissues can be formulated to understand the development and progression of glaucoma.

Declarations

Ethics approval and consent to participate
None to declare.

Competing interests
None to declare.

References

1. Weinreb RN, Khaw PT. Primary open-angle glaucoma. The Lancet. 2004;94221711-1720. https://doi.org/10.1016/S0140-6736(04)16257-0

2. Flammer J, Orgül S, Costa VP, et al. The impact of ocular blood flow in glaucoma. Prog Retin Eye Res. 2002;4359-393. https://doi.org/10.1016/S1350-9462(02)00008-3

3. Anderson DR, Hendrickson A. Effect of intraocular pressure on rapid axoplasmic transport in monkey optic nerve. Invest Ophthalmol Vis Sci. 1974;10771-783.

4. Quigley H, Anderson DR. The dynamics and location of axonal transport blockade by acute intraocular pressure elevation in primate optic nerve. Invest Ophthalmol Vis Sci. 1976;8606-616.

5. Quigley HA, Addicks EM, Green WR, Maumenee AE. Optic nerve damage in human glaucoma: II. The site of injury and susceptibility to damage. Arch Ophthalmol. 1981;4635-649.

6. Wostyn P, De Groot V, Audenaert K, De Deyn PP. Are intracranial pressure fluctuations important in glaucoma? Med Hypotheses. 2011;4598-600. https://doi.org/10.1016/j.mehy.2011.06.043

7. Kaskar OG, Fleischman D, Lee YZ, Thorp BD, Kuznetsov AV, Grace L. Identifying the Critical Factors Governing Translaminar Pressure Differential Through a Compartmental Model. Invest Ophthalmol Vis Sci. 2019;83204-3214. https://doi.org/10.1167/iovs.18-26200

8. Morgan WH, Lind CR, Kain S, Fatehee N, Bala A, Yu D. Retinal vein pulsation is in phase with intracranial pressure and not intraocular pressure. Invest Ophthalmol Vis Sci. 2012;84676-4681. https://doi.org/10.1167/iovs.12-9837

9. Downs JC. Optic nerve head biomechanics in aging and disease. Exp Eye Res. 2015;19-29. https://doi.org/10.1016/j.exer.2015.02.011

10. Jin Y, Wang X, Zhang L, et al. Modeling the origin of the ocular pulse and its impact on the optic nerve head. Invest Ophthalmol Vis Sci. 2018;103997-4010.

11. Bellezza AJ, Hart RT, Burgoyne CF. The optic nerve head as a biomechanical structure: initial finite element modeling. Invest Ophthalmol Vis Sci. 2000;102991-3000.

12. Sigal IA, Flanagan JG, Tertinegg I, Ethier CR. Finite element modeling of optic nerve head biomechanics. Invest Ophthalmol Vis Sci. 2004;124378-4387. https://doi.org/10.1167/iovs.04-0133

13. Sigal IA, Flanagan JG, Ethier CR. Factors influencing optic nerve head biomechanics. Invest Ophthalmol Vis Sci. 2005;114189-4199. https://doi.org/10.1167/iovs.05-0541

14. Sigal IA, Flanagan JG, Tertinegg I, Ethier CR. Modeling individual-specific human optic nerve head biomechanics. Part I: IOP-induced deformations and influence of geometry. Biomech Model Mechanobiol. 2009;285-98. https://doi.org/10.1007/s10237-008-0120-7

15. Sigal IA, Flanagan JG, Tertinegg I, Ethier CR. Modeling individual-specific human optic nerve head biomechanics. Part II: influence of material properties. Biomech Model Mechanobiol. 2009;299-109. https://doi.org10.1007/s10237-008-0119-0

16. Norman RE, Flanagan JG, Sigal IA, Rausch SM, Tertinegg I, Ethier CR. Finite element modeling of the human sclera: influence on optic nerve head biomechanics and connections with glaucoma. Exp Eye Res. 2011;14-12. https://doi.org/10.1016/j.exer.2010.09.014

17. Leung LK, Ko MW, Lam DC. Effect of age-stiffening tissues and intraocular pressure on optic nerve damages. Molecular and Cellular Biomechanics. 2012;2157. https://doi.org/10.3970/mcb.2012.009.157

18. Kharmyssov C, Abdildin YG, Kostas KV. Optic nerve head damage relation to intracranial pressure and corneal properties of eye in glaucoma risk assessment. Med Biol Eng Comput. 2019;71591-1603.

19. Feola AJ, Myers JG, Raykin J, et al. Finite element modeling of factors influencing optic nerve head deformation due to intracranial pressure. Invest Ophthalmol Vis Sci. 2016;41901-1911. https://doi.org/10.1167/iovs.15-17573

20. Wang X, Rumpel H, Lim WEH, et al. Finite element analysis predicts large optic nerve head strains during horizontal eye movements. Invest Ophthalmol Vis Sci. 2016;62452-2462. https://doi.org/10.1167/iovs.15-18986

21. Hua Y, Tong J, Ghate D, Kedar S, Gu L. Intracranial pressure influences the behavior of the optic nerve head. J.Biomech.Eng. 2017;3031003. https://doi.org/10.1115/1.4035406

22. Shin A, Yoo L, Park J and Demer JL. Finite element biomechanics of optic nerve sheath traction in adduction. J Biomech Eng. 2017;10101010. https://doi.org/10.1115/1.4037562

23. Hua Y, Voorhees AP, Sigal IA. Cerebrospinal fluid pressure: revisiting factors influencing optic nerve head biomechanics. Invest Ophthalmol Vis Sci. 2018;1154-165. https://doi.org/10.1167/iovs.17-22488

24. Tong J, Ghate D, Kedar S and Gu L. Relative Contributions of Intracranial Pressure and Intraocular Pressure on Lamina Cribrosa Behavior. J Ophthalmol. 2019 Mar 17;2019:3064949. https://doi.org/10.1155/2019/3064949

25. Muñoz-Sarmiento DM, Rodríguez-Montaño ÓL, Alarcón-Castiblanco JD, Gamboa-Márquez MA, Corredor-Gómez JP, Cortés-Rodríguez CJ. A finite element study of posterior eye biomechanics: The influence of intraocular and cerebrospinal pressure on the optic nerve head, peripapillary region, subarachnoid space and meninges. Informatics in Medicine Unlocked. 2019;100185. https://doi.org/10.1016/j.imu.2019.100185

26. Hasenfratz G . Experimental studies on the display of the optic nerve. In: Ossoinig KC, editor. Ophthalmic echography. The Hague: Martinus Nijhoff/W Junk, 1987:587–602.

27. Reina MA, Casasola ODL, López A, De Andrés JA, Mora M and Fernández A. The origin of the spinal subdural space: ultrastructure findings. Anesthesia & Analgesia. 2002;4991-995. https://doi.org/10.1097/00000539-200204000-00040

28. Schultz DS, Lotz JC, Lee SM, Trinidad ML, Stewart JM. Structural factors that mediate scleral stiffness. Invest Ophthalmol Vis Sci. 2008;104232-4236. https://doi.org/10.1167/iovs.08-1970

29. Spoerl E, Boehm AG, Pillunat LE. The influence of various substances on the biomechanical behavior of lamina cribrosa and peripapillary sclera. Invest Ophthalmol Vis Sci. 2005;41286-1290. https://doi.org/10.1167/iovs.04-0978

30. Hou R, Zhang Z, Yang D, et al. Intracranial pressure (ICP) and optic nerve subarachnoid space pressure (ONSP) correlation in the optic nerve chamber: the Beijing Intracranial and Intraocular Pressure (iCOP) study. Brain Res. 2016;201-208. https://doi.org/10.1016/j.brainres.2016.01.011

31. Morgan WH, Yu D, Cooper RL, Alder VA, Cringle SJ, Constable IJ. The influence of cerebrospinal fluid pressure on the lamina cribrosa tissue pressure gradient. Invest Ophthalmol Vis Sci. 1995;61163-1172.

32. Morgan WH, Yu D, Alder VA, et al. The correlation between cerebrospinal fluid pressure and retrolaminar tissue pressure. Invest Ophthalmol Vis Sci. 1998;81419-1428.

33. Liu D, Kahn M. Measurement and relationship of subarachnoid pressure of the optic nerve to intracranial pressures in fresh cadavers. Am J Ophthalmol. 1993;5548-556. https://doi.org/10.1016/S0002-9394(14)73195-2

34. Moller PM. The pressure in the orbit. Acta Ophthalmol. 1955;Suppl 431-100.

35. Sommer A. Intraocular pressure and glaucoma. Am J Ophthalmol. 1989;2186-188.

36. Heijl A, Leske MC, Bengtsson B, Hyman L, Bengtsson B, Hussein M. Reduction of intraocular pressure and glaucoma progression: results from the Early Manifest Glaucoma Trial. Arch Ophthalmol. 2002;101268-1279.

37. Siaudvytyte L, Januleviciene I, Daveckaite A, et al. Literature review and meta-analysis of translaminar pressure difference in open-angle glaucoma. Eye. 2015;101242-1250.

38. Jonas JB, Berenshtein E and Holbach L. Anatomic relationship between lamina cribrosa, intraocular space, and cerebrospinal fluid space. Invest Ophthalmol Vis Sci. 2003;125189-5195. https://doi.org/10.1167/iovs.03-0174

39. Burgoyne CF. A biomechanical paradigm for axonal insult within the optic nerve head in aging and glaucoma. Exp Eye Res. 2011;2120-132.

40. Jay JL, Murdoch JR. The rate of visual field loss in untreated primary open angle glaucoma. Br J Ophthalmol. 1993;3176-178.

41. Leske MC, Connell AM, Wu S, et al. Incidence of open-angle glaucoma: the Barbados Eye Studies. Arch Ophthalmol. 2001;189-95.

42. Grytz R, Girkin CA, Libertiaux V, Downs JC. Perspectives on biomechanical growth and remodeling mechanisms in glaucoma. Mech Res Commun. 2012;92-106.

43. Albon J, Purslow PP, Karwatowski WS, Easty DL. Age related compliance of the lamina cribrosa in human eyes. Br J Ophthalmol. 2000;3318-323.

44. Geraghty B, Jones SW, Rama P, Akhtar R, Elsheikh A. Age-related variations in the biomechanical properties of human sclera. J Mech Behav Biomed Mater. 2012;181-191. https://doi.org/10.1016/j.jmbbm.2012.10.011

45. Albon J, Karwatowski WS, Avery N, Easty DL, Duance VC. Changes in the collagenous matrix of the aging human lamina cribrosa. Br J Ophthalmol. 1995;4368-375.

46. Simo JC. On a fully three-dimensional finite-strain viscoelastic damage model: formulation and computational aspects. Comput Methods Appl Mech Eng. 1987;2153-173.

47. Rodríguez JF, Cacho F, Bea JA, Doblaré M. A stochastic-structurally based three dimensional finite-strain damage model for fibrous soft tissue. J Mech Phys Solids. 2006;4864-886.

48. Martin C, Sun W. Modeling of long-term fatigue damage of soft tissue with stress softening and permanent set effects. Biomech Model Mechanobiol. 2013;4645-655.

49. Downs JC, Burgoyne CF, Seigfried WP, Reynaud JF, Strouthidis NG, Sallee V. 24-hour IOP telemetry in the nonhuman primate: implant system performance and initial characterization of IOP at multiple timescales. Invest Ophthalmol Vis Sci. 2011;107365-7375. https://doi.org/10.1167/iovs.11-7955

50. Resta V, Novelli E, Vozzi G, et al. Acute retinal ganglion cell injury caused by intraocular pressure spikes is mediated by endogenous extracellular ATP. Eur J Neurosci. 2007;92741-2754. https://doi.org/10.1111/j.1460-9568.2007.05528.x

51. Caprioli J, Coleman AL. Intraocular pressure fluctuation: a risk factor for visual field progression at low intraocular pressures in the Advanced Glaucoma Intervention Study. Ophthalmology. 2008;71123-1129. e3. https://doi.org/10.1016/j.ophtha.2007.10.031

52. Hong S, Seong GJ, Hong YJ. Long-term intraocular pressure fluctuation and progressive visual field deterioration in patients with glaucoma and low intraocular pressures after a triple procedure. Arch Ophthalmol. 2007;81010-1013. https://doi.org/10.1001/archopht.125.8.1010

53. Kim JH, Caprioli J. Intraocular pressure fluctuation: is it important? J Ophthalmic Vis Res. 2018;2170. https://doi.org/10.4103/jovr.jovr_35_18

54. Guo Z, Chang K, Wei X. Intraocular pressure fluctuation and the risk of glaucomatous damage deterioration: a meta-analysis. Int J Ophthalmol. 2019;1123. https://doi.org/10.18240/ijo.2019.01.19

55. Matlach J, Bender S, König J, Binder H, Pfeiffer N, Hoffmann EM. Investigation of intraocular pressure fluctuation as a risk factor of glaucoma progression. Clin Ophthalmol. 2019;9. https://doi.org/10.2147/OPTH.S186526

56. Asrani S, Zeimer R, Wilensky J, Gieser D, Vitale S, Lindenmuth K. Large diurnal fluctuations in intraocular pressure are an independent risk factor in patients with glaucoma. J Glaucoma. 2000;2134-142. https://doi.org/10.1097/00061198-200004000-00002

57. Jonas JB, Budde WM, Stroux A, Oberacher-Velten IM, Jünemann A. Diurnal intraocular pressure profiles and progression of chronic open-angle glaucoma. Eye. 2007;7948-951.

58. Lee YR, Kook MS, Joe SG, et al. Circadian (24-hour) pattern of intraocular pressure and visual field damage in eyes with normal-tension glaucoma. Invest Ophthalmol Vis Sci. 2012;2881-887.

59. Wostyn P, De Groot V, Van Dam D, Audenaert K, De Deyn PP. Intracranial pressure fluctuations: a potential risk factor for glaucoma. Acta Ophthalmol. 2015;1e83-e84. https://doi.org/10.1111/aos.12331

60. McMonnies CW. The interaction between intracranial pressure, intraocular pressure and lamina cribrosal compression in glaucoma. Clin Exp Optom. 2016;3219-226. https://doi.org/10.1111/cxo.12333

61. Downs JC, Girkin CA. Lamina cribrosa in glaucoma. Curr Opin Ophthalmol. 2017;2113. https://doi.org/10.1097/ICU.0000000000000354

62. Kirwan RP, Fenerty CH, Crean J, Wordinger RJ, Clark AF, O'Brien CJ. Influence of cyclical mechanical strain on extracellular matrix gene expression in human lamina cribrosa cells in vitro. Mol Vis. 2005;798e810.

63. Coudrillier B, Boote C, Quigley HA, Nguyen TD. Scleral anisotropy and its effects on the mechanical response of the optic nerve head. Biomechanics and modeling in mechanobiology. 2013;5941-963.

64. Pijanka JK, Coudrillier B, Ziegler K, et al. Quantitative mapping of collagen fiber orientation in non-glaucoma and glaucoma posterior human sclerae. Invest Ophthalmol Vis Sci. 2012;95258-5270.

65. Zhang W, Liu Y, Kassab GS. Viscoelasticity reduces the dynamic stresses and strains in the vessel wall: implications for vessel fatigue. Am J Physiol Heart Circ Physiol. 2007;4H2355-H2360.